



Nonlinear adaptive control of pitch for parameter uncertain twin rotor mechanism

Ahmad Naseer, Muhammad R. Ehsan, Usman Ali

Department of Electrical Engineering, COMSATS Institute of Information Technology, Wah-47040, Pakistan

Abstract A twin rotor system is a static testbed to simulate and control certain dynamics of rotor craft aerial vehicles. The control of pitch dynamics of a twin rotor mechanism using nonlinear adaptive control method has been considered. The system parameters are assumed unknown and the technique of nonlinear adaptation using manifold immersion is performed for their estimation. Reference tracking is obtained. The experimental validation of the theoretically proposed controller is presented by implementing discrete time realization of control algorithm using digital controller interfaced in real time with Simulink. The potential of proposed algorithm relies upon the flexibility in the structure of control algorithm and promising transient behavior of closed loop system dynamics.

Keywords Twin Rotor System, Adaptive Control, Manifold Immersion, Parameter Estimation

1. Introduction

A twin rotor system is a platform that is used to simulate certain system dynamics found in the helicopters and other rotor crafts. This piece of equipment behaves as a static test bed for many aerial vehicles. It is a challenging system for modelling and control. It also acts as a benchmark to simulate and test new and advanced control techniques. A twin rotor mechanism is two degree of freedom system. It has pitch dynamics and roll dynamics, either of which are nonlinear and mutually coupled. Moreover, including in the dynamics of the motor-propeller actuator along with the motor amplifier, complicates the problem still more as it adds more state variables in system dynamics, which tantamount to increase in the order of the system. To add to the difficulty, there are various uncertain system parameters. Hence there is always a room for the better and effective control technique for twin rotor mechanism.

There are various control techniques applied to twin rotor mechanism in literature. A nonlinear robust controller is designed for the twin rotor control system (TRCS) in [1], where the proposed controller is designed using dynamic surface control (DSC) technique, which is an advance version of integral Back-Stepping control approach through the use of dynamic low pass filters. The work in [2] focuses on the research of practical application of robust suboptimal control for the Twin Rotor multiple input multiple output (MIMO) System, where the MIMO system is represented as dynamically related single input single output (SISO) systems. The robust and suboptimal control algorithm is based on the auxiliary loop method for disturbances compensation and suboptimal linear quadratic regulator (LQR), which is applied to the simplified linearized model of the plant. The research in [3] considers a model based switching control scheme. The philosophy of the approach is to design a conventional linear or nonlinear feedback control scheme for a nominal plant model and to force the true system states to that of the nominal model by introducing a switching term. Model predictive control and passivity based control algorithm is proposed in [4, 5], which rely upon solving an optimization problem (OP) in order to minimize some user defined objective function (OF) subjected to constraints on the characteristic variables and energy shaping and damping injection (ESDI) techniques. Neuro sliding mode controller and Nonlinear robust observer based control are considered in [6, 7] and Adaptive Sliding Mode Tracking Control is used in [8].



Most of these techniques consider the linear system model or a reduced order model of the system such as explicitly stated in [2]. Moreover, controllers do not have many tunable parameters to gain much control over system responses. Many controllers suffer degradation of response as the operation conditions change or the system parameters vary with time. We have applied a robust adaptive nonlinear control algorithm that relies on robustification of reduced order system controller against full order system dynamics [9]. The controller is also robust against unknown system parameters and has a lot of free tunable parameters to gain control over feedback dynamic response of the system output.

2. Overview of the Hardware Setup

Figure 1 shows the schematic diagram of the hardware setup. It consists of two rotors. One of the rotors actuates pitch dynamics and it is termed the main rotor. The other rotor actuates yaw dynamics and it is termed the tail rotor. These actuators consist of brushless DC motor-propeller assemblies connected to a rod that is mounted on a pillar-base support. Motors are driven by electronic speed controller. The hardware has two potentiometers to measure pitch and yaw angles. There is an adjustable counter weight in the assembly.

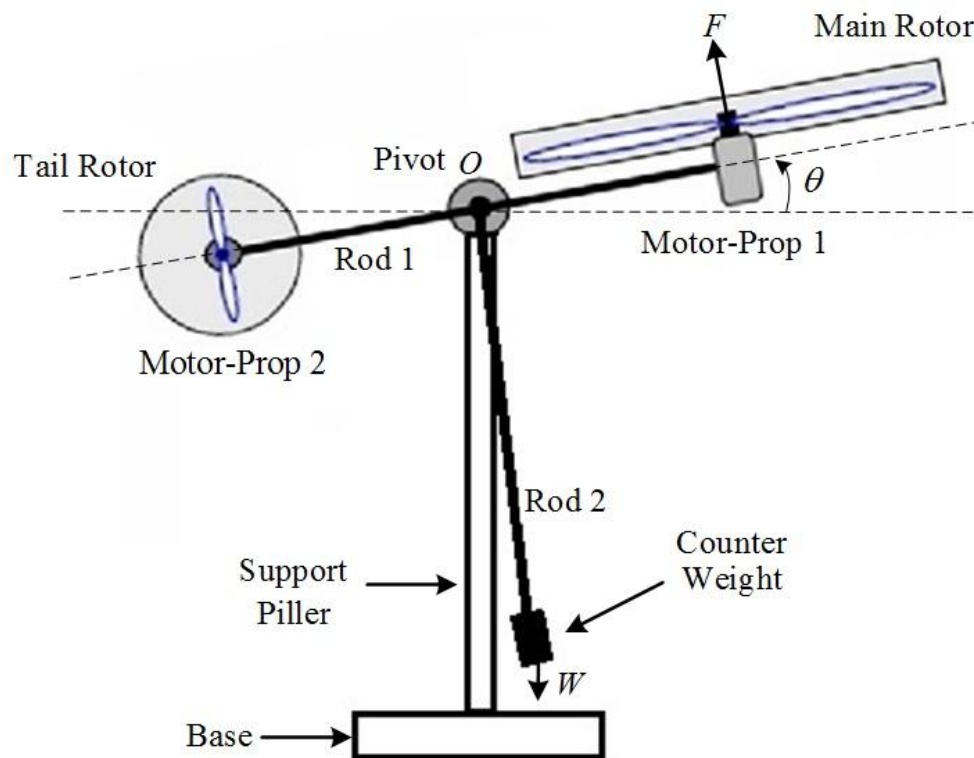


Figure 1: An overview of the hardware setup.

3. The Control Algorithm Synthesis

Consider a nonlinear parameter uncertain system,

$$\dot{\underline{p}} = \underline{s}(\underline{p}, u_e) = \underline{f}(\underline{p}) + \underline{g}(\underline{p})u_e \quad (1)$$

where $\underline{p} \in \mathbb{R}^n$ and $u_e \in \mathbb{R}^m$. The state vector \underline{p} evolves on a smooth manifold P of dimension n , which is spanned by tangential manifold to the system map \underline{s} . The system map \underline{s} in Equation 1 has been decomposed into a drift vector field $\underline{f}(\cdot)$ and a controlled vector field \underline{g} . In Equation 1, $u_e \in U(\underline{p})$ is the system forcing function with U a state dependent input set which belongs to the control bundle $\bigcup_{\underline{p} \in P} U(\underline{p})$. The topological manifold immersion based nonlinear control approach involves defining a reduced order exosystem. The state



trajectories of the exosystem evolve on a C^∞ submanifold $Q \subset P$. The problem of controller design then boiled down to synthesize a control law that dynamically immerses the state trajectories of full order system to the manifold Q . Let us consider an exosystem with state vector $\underline{q} \in \mathbb{R}^q$ with $q < n$, which contains origin in its reachable set. This can be achieved by defining the vector field $\underline{Y}(\underline{q})$ of the exosystem that governs the evolution of \underline{q} as given by Equation 2.

$$\dot{\underline{q}} = \underline{Y}(\underline{q}) \quad (2)$$

Defining a smooth submanifold for the exosystem of Equation 2 as:

$$Q = \left\{ \underline{p} \in \mathbb{R}^n \mid \underline{p} = \underline{\psi}(\underline{q}); \underline{q} \in \mathbb{R}^q \right\} \quad (3)$$

The controlled integral curves of system map \underline{s} can be attracted by the submanifold Q if partial differential Equation 4 along with the condition in Equation 5 is satisfied [9].

$$\underline{f}(\underline{\psi}(\underline{q})) + \underline{g}(\underline{\psi}(\underline{q}))\rho(\underline{\psi}) = L_{\underline{r}}\underline{\psi} \quad (4)$$

$$\underline{q}(t) = \underline{0} \quad \forall \underline{q}(0) \in \mathbb{R}^2 \text{ as } t \rightarrow \infty \quad (5)$$

Here $L_{\underline{r}}\underline{\psi} = (\nabla_{\underline{q}}\underline{\psi})\underline{Y}(\underline{q})$ is the so-called Lie derivative. Also $\rho(\underline{\psi}(\underline{q})) = v(\underline{\psi}(\underline{q}), 0)$ on the submanifold Q and $u = v(\underline{p}, \zeta(\underline{p}))$ is the synthesized feedback control law that renders Q attractive. $\zeta(\cdot)$ is the implicit description of Q and it is given by parameterized form in Equation 6.

$$\zeta(\underline{p}) = \underline{p} - \underline{\psi}(\underline{q}) = 0 \quad (6)$$

Introducing state variable \underline{h} to define “off” the submanifold Q dynamics given by:

$$\dot{\underline{h}} = L_{\underline{s}}\zeta \Big|_{u=\mathcal{G}(\underline{p}, \underline{h})} = \left(\frac{\partial \zeta}{\partial \underline{q}} \right) \underline{s}(\underline{p}, \mathcal{G}(\underline{p}, \underline{h})) \quad (7)$$

In terms of \underline{h} and any constant $\alpha > 0$, the synthesized controller \mathcal{G} the system mapping is given by,

$$\dot{\underline{p}} = \underline{s}(\underline{p}, \mathcal{G}(\underline{p}, \underline{h})) \quad (8)$$

For any general system of form,

$$\begin{aligned} \dot{\underline{p}}_1 &= \underline{\xi}_1(\underline{p}_1) + \underline{\xi}_2(\underline{p}_1)\underline{p}_2 \\ \dot{\underline{p}}_2 &= \underline{\varphi}(\underline{p})^T \underline{\lambda}_1 + \underline{\lambda}_2 u \end{aligned} \quad (9)$$

where $\underline{\xi}_i(\cdot)$ and $\underline{\varphi}(\cdot)$ are smooth mappings, $\underline{\lambda}_i$ are unknown parameters and $\dot{\underline{p}}_1 = \underline{\xi}_1(\underline{p}_1)$ is globally stable, then for constants $\varepsilon > 0$ and $k > 0$, the geometric adaptive estimates of $\underline{\lambda}_i$ are given by [9].

$$\dot{\hat{\underline{\lambda}}} = - \left(I + \nabla_{\hat{\underline{\lambda}}} \underline{v} \right)^{-1} \begin{pmatrix} \left(\nabla_{\underline{p}_1} \underline{v} \right) \left(\underline{\xi}_1(\underline{p}_1) + \underline{\xi}_2(\underline{p}_1)\underline{p}_2 \right) \\ + \frac{\partial \underline{v}}{\partial \underline{p}_2} \left(-k\underline{p}_2 - \varepsilon L_{\underline{\xi}_2} V_1(\underline{p}_1) \right) \end{pmatrix} \quad (10)$$

and the corresponding geomantic synthesized control law is given by,

$$u = - \left(\hat{\underline{\lambda}}_2 + \underline{v}_2(\underline{p}, \hat{\underline{\lambda}}_1) \right) \begin{pmatrix} k\underline{p}_2 + \varepsilon L_{\underline{\xi}_2} V_1(\underline{p}_1) \\ + \underline{\varphi}(\underline{p})^T \left(\hat{\underline{\lambda}}_1 + \underline{v}_1(\underline{p}) \right) \end{pmatrix} \quad (11)$$



The vector $\underline{v} = [\underline{v}_1(\underline{p}) \quad \underline{v}_2(\underline{p}, \hat{\lambda}_1)]^T$ is given by:

$$\underline{v}_1(\underline{p}) = \gamma_1 \int_0^{p_2} \varphi(\underline{p}_1, \eta) d\eta \tag{12}$$

$$\begin{aligned} \underline{v}_2(\underline{p}, \hat{\lambda}_1) = \gamma_2 \left(k \frac{p_2}{2} + \varepsilon L_{\xi_2} V_1(\underline{p}_1) p_2 \right) \\ + \gamma_2 \int_0^{p_2} \varphi(\underline{p}_1, \eta)^T (\hat{\lambda}_1 + \underline{v}_1(\underline{p}_1, \eta)) d\eta \end{aligned} \tag{13}$$

According to [10], $V_1(\underline{p}_1)$ is any mapping such that for some class-K function $\kappa(\cdot)$, we have,

$$L_{\xi_1} V_1(\underline{p}_1) \leq -\kappa(\underline{p}_1) \tag{14}$$

and $\gamma_1 > 0, \gamma_2 > 0$ are constants.

4. Experimental test bed and system dynamics

Consider the experimental testbed of twin rotor mechanism in the Figure 2. If θ denotes pitch angle of main rod and ω denotes the angular speed of main rotor motor then the system state variables for pitch dynamics are described by Equation 15.

$$\underline{p} = [p_1 \quad p_2 \quad p_3]^T = [\theta \quad \dot{\theta} \quad \omega]^T \tag{15}$$

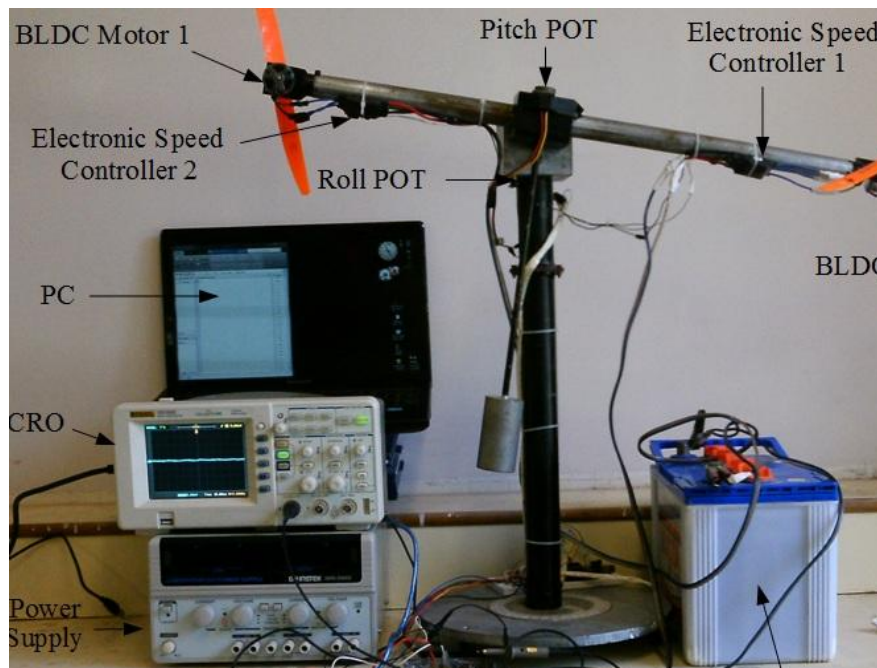


Figure 2: An overview of the experimental setup.

If we consider the second order curve fit for the static thrust calibration of main rotor against its driving signal using arrangement in Figure 3, and results in Figure 4, then the dynamics of system are described by following system of Equation 16. Force decomposition is shown in Figure 5.

$$\begin{aligned} \underline{f}(\underline{p}) &= [p_2 \quad -k_1 p_2 + k_2 p_3^2 \quad -p_3 k_3]^T \\ \underline{g}(\underline{p}) &= [0 \quad 0 \quad k_4]^T \\ \underline{s}(\underline{p}, u_e) &= [p_3 \quad -k_1 p_2 + k_2 p_3^2 \quad -p_3 k_3 + k_4 u_e]^T \end{aligned} \tag{16}$$

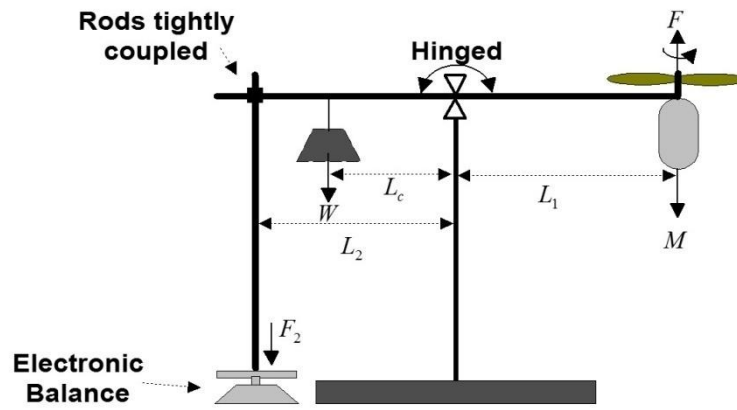


Figure 3: Thrust calibration setup.

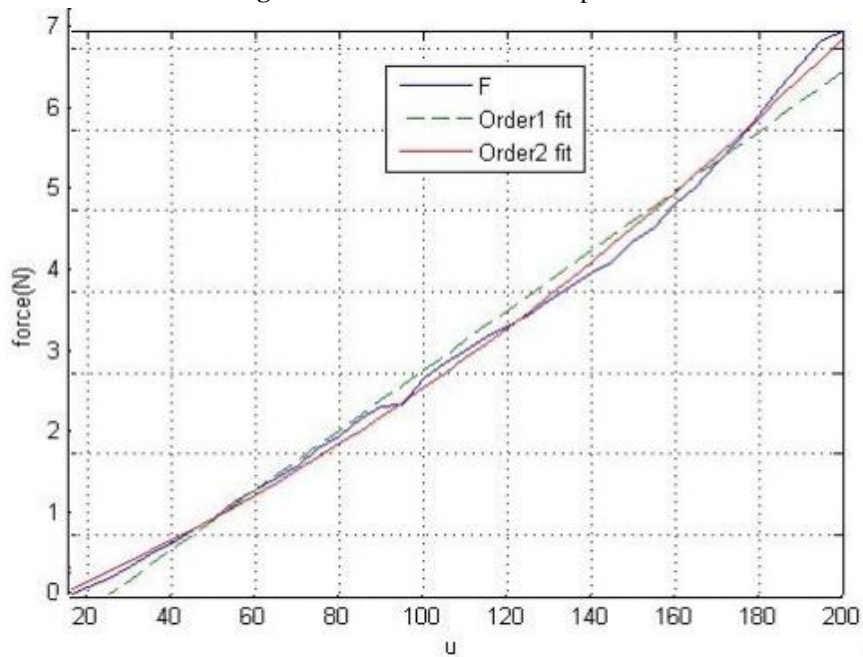


Figure 4: Motor static thrust calibration curve fits.

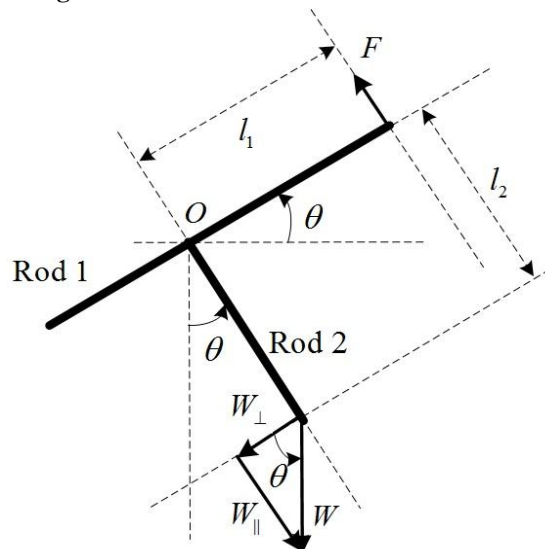


Figure 5: Force decomposition.

Equation 2 and Equation 8 evaluate to following expressions.



$$\underline{Y}(\underline{q}) = [q_2 \quad -k_1 + k_2 \zeta_1^2]^T \quad (17)$$

$$\underline{p} = \underline{\psi}(\underline{q}) = [q_1 \quad q_2 \quad \psi_1(q_1, q_2)]^T \quad (18)$$

$$\mathcal{G}(\underline{p}, \dot{h}) = \frac{-\alpha \dot{h} + \dot{\zeta}_1 + k_3 p_3}{k_4} \quad (19)$$

The reduced order system is given by Equation 20.

$$\begin{aligned} \dot{h} &= -\alpha \dot{h} \\ \dot{p}_1 &= p_2 \\ \dot{p}_2 &= -k_1 p_2 + k_2 \zeta_1^2 \\ \dot{p}_3 &= -\alpha \dot{h} + \dot{\zeta}_1 \end{aligned} \quad (20)$$

The system in Equation 20 immerses to system described by Equation 21.

$$\begin{aligned} \dot{p}_1 &= p_2 \\ \dot{p}_2 &= -k_1 + k_2 \zeta_1^2 \end{aligned} \quad (21)$$

Let us consider feedback linearization of Equation 21 as,

$$\zeta_1 = \sqrt{u} : u > 0 \quad (22)$$

The immersion control law is given by,

$$\mathcal{G}(\underline{p}, \dot{h}) = \frac{-\alpha \dot{h} + \dot{\zeta}_1 + k_3 p_3}{k_4} \quad (23)$$

Using Equation 21 and Equation 22 we get,

$$\dot{\underline{p}} = [p_2 \quad -k_1 p_2 + k_2 u]^T \quad (24)$$

For the estimation of unknown parameters in Equation 24, using the results in Equation 9 through Equation 14, we get.

$$\begin{aligned} \xi_1(p_1) &= 0, \quad \xi_2(p_1) = 1 \\ \lambda_1 &= k_1, \quad \lambda_2 = k_2 > 0 \\ \varphi(\underline{p}) &= -1 \end{aligned} \quad (25)$$

$$L_{\xi_2} V_1(\underline{p}_1) = 2p_1 \quad (26)$$

$$\underline{v} = \begin{bmatrix} c_1 p_2 \\ c_2 p_2^2 + c_3 \hat{\lambda}_1 p_2 + c_4 p_1 p_2 \end{bmatrix} \quad (27)$$

$$\nabla_{\hat{\lambda}} \underline{v} = \begin{bmatrix} 0 & 0 \\ -\gamma_2 p_2 & 0 \end{bmatrix} \quad (28)$$

$$\nabla_{p_1} \underline{v} = \frac{\partial \underline{v}}{\partial p_1} = [0 \quad 2\varepsilon \gamma_2 p_2]^T \quad (29)$$

$$\frac{\partial \underline{v}}{\partial p_2} = [-\gamma_1 \quad k\gamma_2 p_2 + 2\gamma_2 k p_1 - \gamma_2 \hat{\lambda}_1 + \gamma_1 \gamma_2 p_2]^T \quad (30)$$

The parameter estimates in Equation 10 leads us to,

$$\dot{\hat{\lambda}} = \begin{bmatrix} c_5 p_1 + c_6 p_2 \\ c_7 p_1^2 + c_8 p_2^2 + c_9 p_1 p_2 + c_{10} p_2 \hat{\lambda}_1 + c_{11} p_1 \hat{\lambda}_1 \end{bmatrix} \quad (31)$$



The control law in terms of estimates parameters is given by,

$$u = -(\hat{\lambda}_2 + v_2(\underline{p}, \hat{\lambda}_1)) (kp_2 + 2\varepsilon p_1 - \hat{\lambda}_1 - v_1(\underline{p})) \tag{32}$$

At the last the reference tracking is achieved by modifications of control law as,

$$g_1(\underline{p}, \hat{h}) = \frac{-\alpha \hat{h} + \dot{\zeta}_1 + k_3 p_3}{k_4} + \sigma(t) \tag{33}$$

A typical classical proportional derivative tracker law can be used to follow reference command as given by,

$$\sigma(t) = \Xi(e(t)) \tag{34}$$

$$\Xi(.) = -\frac{k_3}{k_4} \left(k_p(.) + k_d \frac{d(.)}{dt} \right) \tag{35}$$

5. Simulation and Experimental Testing

The actual values of the system parameters in the system modelling equations are given in Table 1.

Table 1: Numerical values of the system parameters.

Parameter	Value	Parameter	Value
k_3	145	c_4	0.018
k_4	7.15	c_5	-0.25
k	61	c_6	-214
γ_1	4.1	c_7	5×10^{-4}
γ_2	1.0	c_8	845.0
ε	2.1×10^{-3}	c_9	0.25
c_1	-6.25	c_{10}	-750.0
c_2	72.0	c_{11}	-0.05
c_3	-3.25	c_{12}	0.125

The Simulink model of the closed loop system with reference tracker is shown in Figure 6.

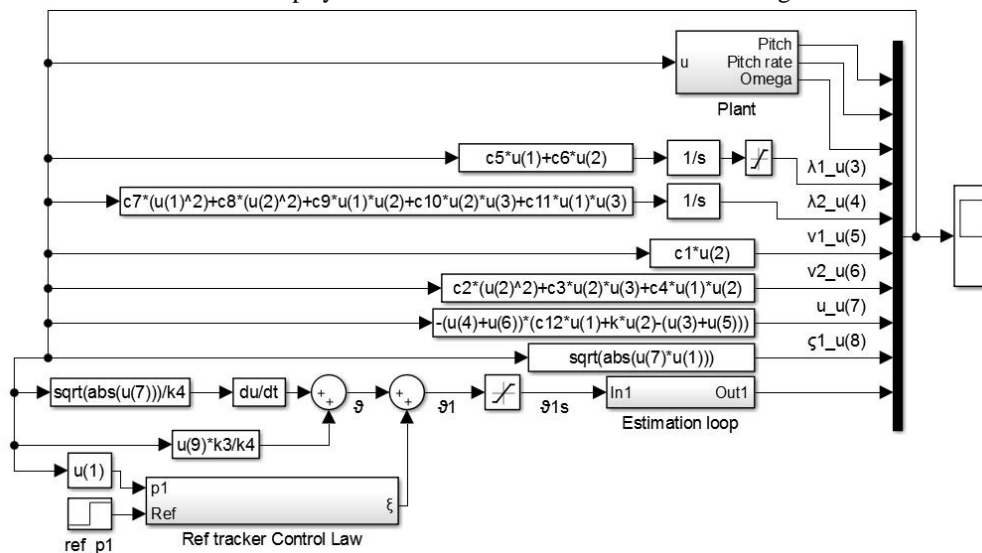


Figure 6: Simulink model of the closed loop system

The simulation result for pitch response is shown in Figure 7. The response is stable with zero steady state error.

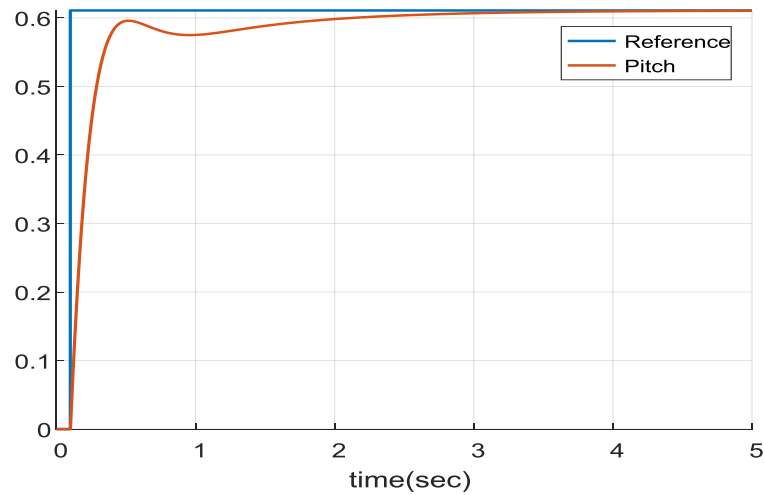


Figure 7: Closed loop simulation response of Twin Rotor Pitch.

The simulation result for pitch rate response is shown in Figure 8. The pitch rate decays to zero within 1.5 seconds.

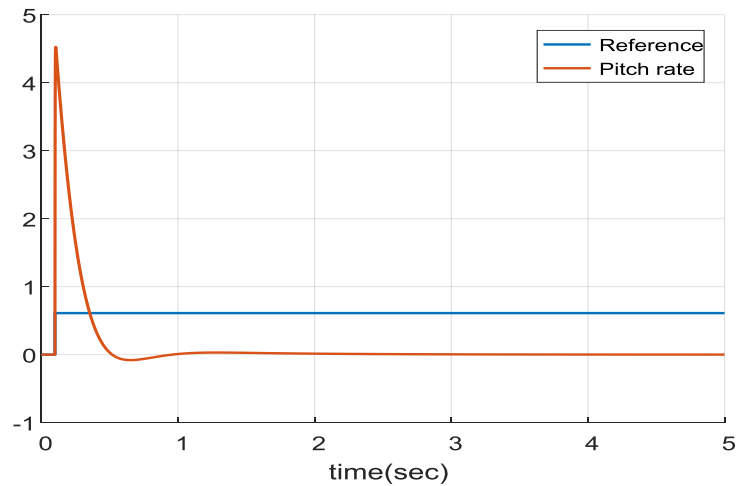


Figure 8: Closed loop simulation response of Twin Rotor Pitch Rate.

The simulation result for manipulated variable response is shown in Figure 9. The magnitude of variable is within practical limits and drives the plant output to the desired reference signal.

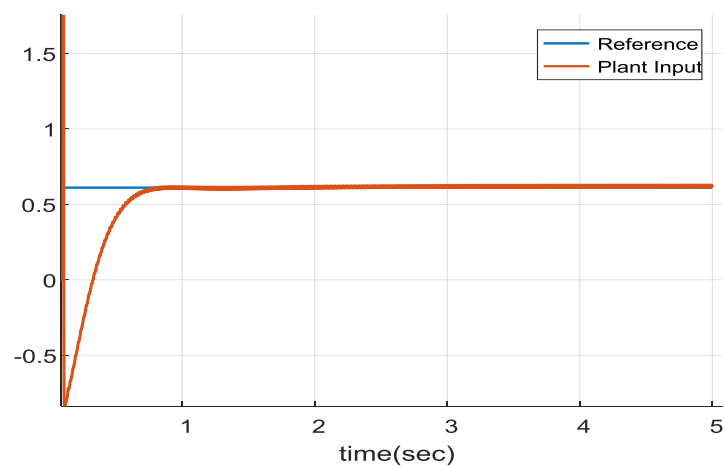


Figure 9: Closed loop simulation response manipulated variable.



The schematic representation of experimental hardware setup is shown in Figure 10.

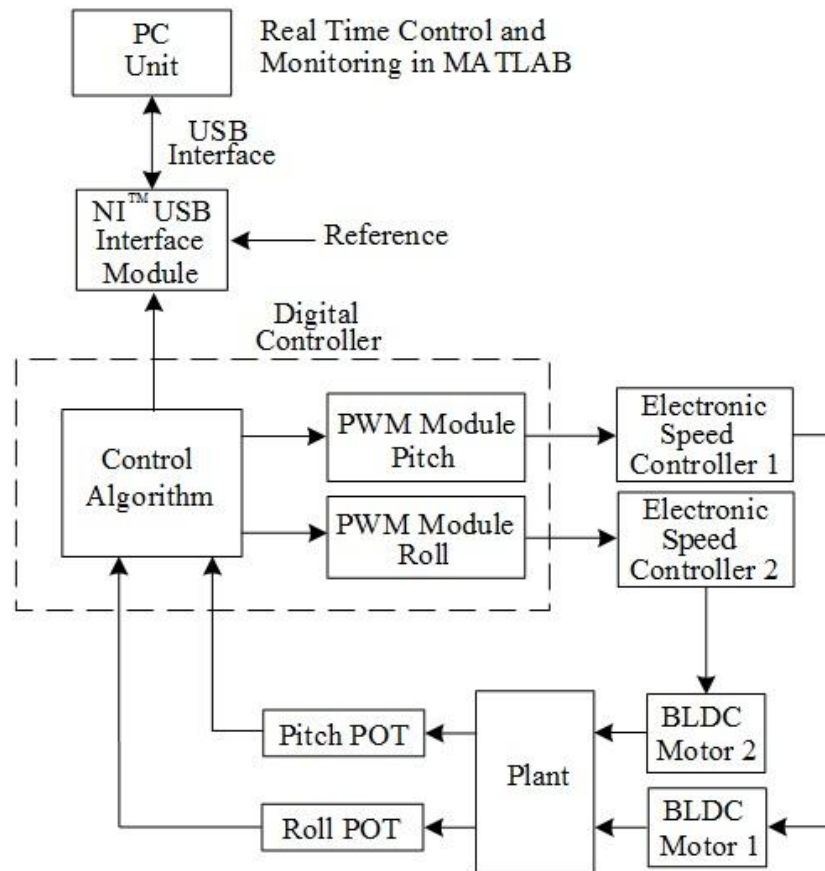


Figure 10: Schematic representation of hardware setup.

The experimental RCP Simulink model of the closed loop system with reference tracker is shown in Figure 11.

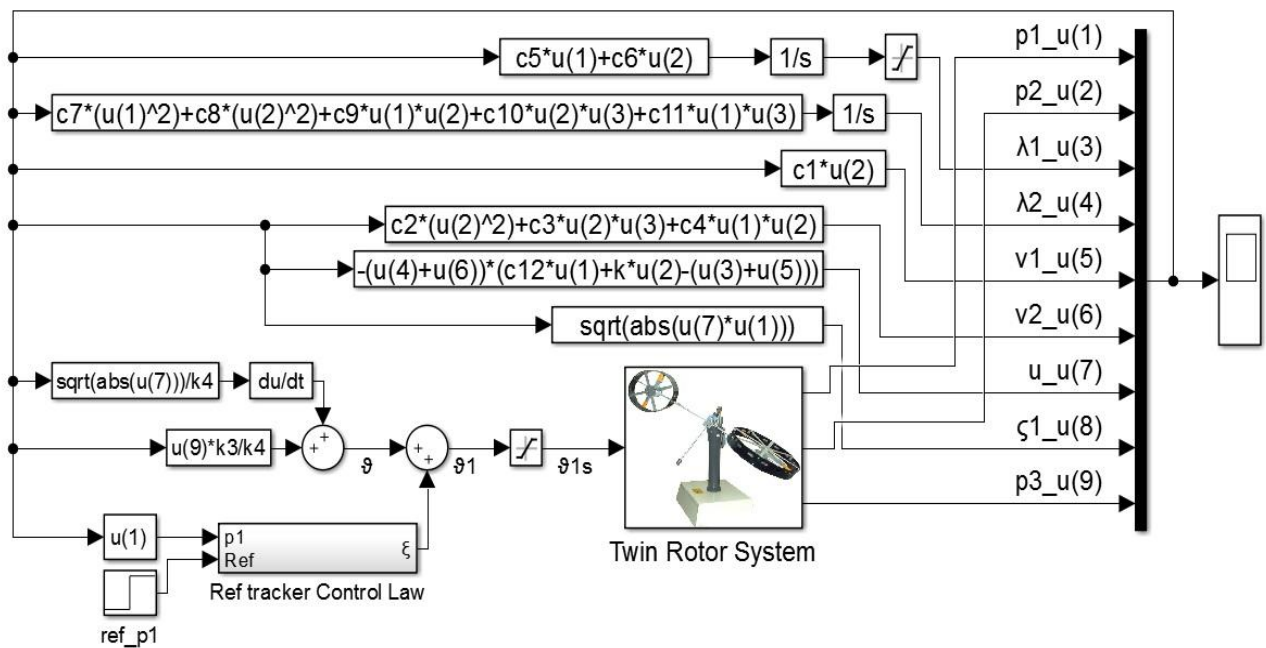


Figure 11: RCP mode of operation of testbed

The experimental result for pitch response is shown in Figure 12. The response is stable with zero steady state error.

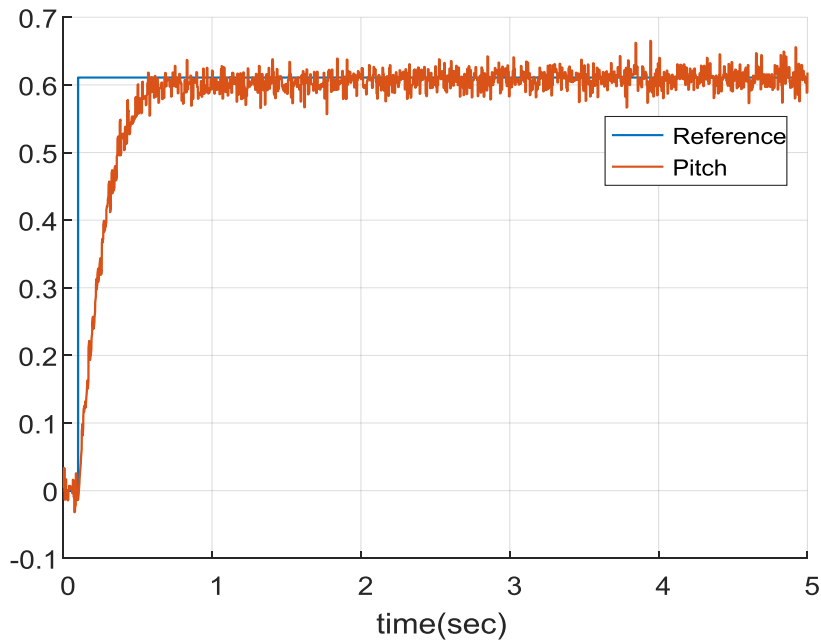


Figure 12: Experimental closed loop response of Twin Rotor Pitch.

The experimental result for pitch rate response is shown in Figure 13. The pitch rate decays to zero within 1.5 seconds.

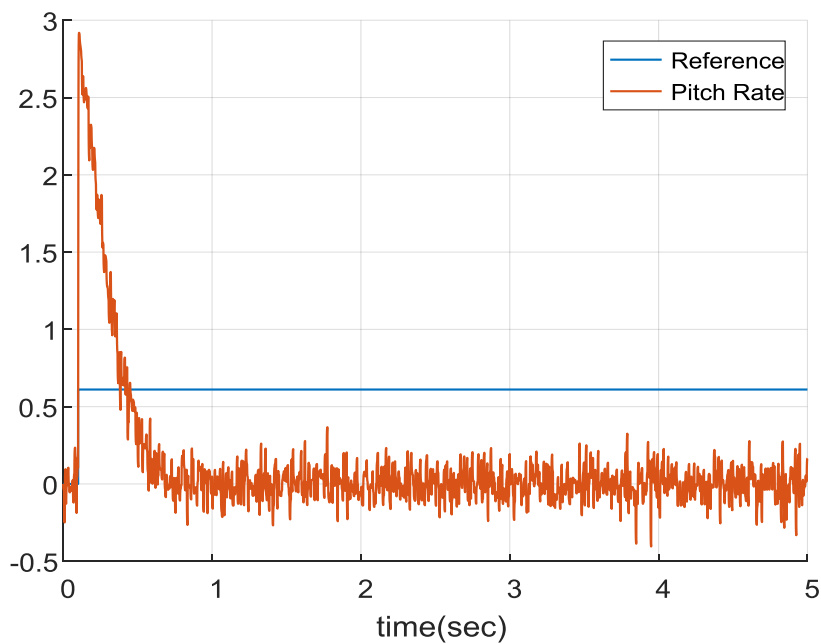


Figure 13: Experimental closed loop response of Twin Rotor Pitch Rate.

The experimental result for manipulated variable response is shown in Figure 14. The magnitude of variable is within practical limits and drives the plant output to the desired reference signal.



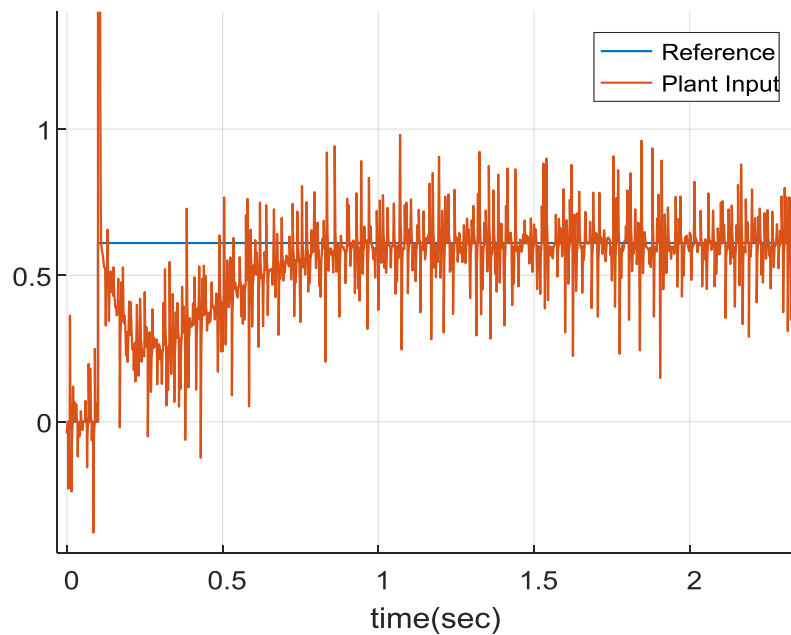


Figure 14: Experimental closed loop response of manipulated variable.

6. Discussion and Conclusions

A robust nonlinear adaptive controller for the pitch of twin rotor mechanism has been presented. System parameters are considered unknown and they are estimated using nonlinear manifold immersive adaptation. The proposed control technique is simulated in Simulink. The theoretical technique is tested in real time using digital controllers and data acquisition cards. The control algorithm has a lot of free tunable parameters. The results showed promising behavior of closed loop system in the presence of parameters uncertainties. Moreover, a greater control of closed loop system dynamics is possible owing to the flexibility in control algorithm.

References

- [1]. Sharma, J., & Pratap, B. (2016). Nonlinear robust dynamic surface controller design for twin rotor control system. *IEEE 1st International Conference on Power Electronics, Intelligent Control and Energy Systems (ICPEICES)*, 1:1-6.
- [2]. Vrazevsky, S. A., Chugina, J. V., Furtat, I. B., & Kremlev, A. S. (2016). Robust suboptimal output control for a Twin Rotor MIMO System. *8th International Congress on Ultra Modern Telecommunications and Control Systems and Workshops*, 1:23-28.
- [3]. Efe, M. O. (2016). Nominal model based switching control of a twin rotor system. *42nd Annual Conference of the IEEE Industrial Electronics Society*, 1:241-246.
- [4]. Dutescu, D. A., Radac M. B., & Precup, R. E. (2017). Model predictive control of a nonlinear laboratory twin rotor aero-dynamical system. *15th International Symposium on Applied Machine Intelligence and Informatics*, 1:37-42.
- [5]. Mustafa, G., & N. Iqbal, N. (2004). Passivity Based Control of Two Degrees of Freedom Twin Rotor Control System. *Student Conference on Engineering, Sciences and Technology*, 1:112-115.
- [6]. Pratap, B. (2012). Neuro sliding mode controller for twin rotor control system. *Students Conference on Engineering and Systems*, 1:1-5.
- [7]. Singh, A. P., & Pratap, B. (2015). Nonlinear robust observer based control of twin rotor control system with friction. *International Conference on Signal Processing, Computing and Control*, 1:173-178.
- [8]. Nguyen, V. C. (2015). Adaptive Sliding Mode Tracking Control For Twin Rotor Multi-input Multi-output Nonlinear System. *International journal of control, automation and systems*, 4(4):9-16.



- [9]. Astolfi, A., & Ortega, R. (2003). Immersion and invariance: a new tool for stabilization and adaptive control of nonlinear systems. *IEEE Transactions on Automatic Control*, 48(4):590–606.
- [10]. Jurdjevic, V. (1996). *Geometric Control Theory*. Cambridge University Press. Cambridge, UK

